

Highly resistive epitaxial Mg-doped GdN thin films

C.-M. Lee, H. Warring, S. Vézian, B. Damilano, S. Granville, M. Al Khalfioui, Y. Cordier, H. J. Trodahl, B. J. Ruck, and F. Natali

Citation: [Applied Physics Letters](#) **106**, 022401 (2015); doi: 10.1063/1.4905598

View online: <http://dx.doi.org/10.1063/1.4905598>

View Table of Contents: <http://scitation.aip.org/content/aip/journal/apl/106/2?ver=pdfcov>

Published by the [AIP Publishing](#)

Articles you may be interested in

[Growth and characterization of Sc-doped EuO thin films](#)

Appl. Phys. Lett. **104**, 052403 (2014); 10.1063/1.4863752

[Study of Gd-doped Bi₂Te₃ thin films: Molecular beam epitaxy growth and magnetic properties](#)

J. Appl. Phys. **115**, 023904 (2014); 10.1063/1.4861615

[Room-temperature ferromagnetism in epitaxial Mg-doped SnO₂ thin films](#)

Appl. Phys. Lett. **100**, 182405 (2012); 10.1063/1.4711220

[Influence of the substrate temperature on the Curie temperature and charge carrier density of epitaxial Gd-doped EuO films](#)

Appl. Phys. Lett. **98**, 102110 (2011); 10.1063/1.3563708

[Magnetic properties of epitaxial Co-doped anatase TiO₂ thin films with excellent structural quality](#)

J. Vac. Sci. Technol. B **24**, 2012 (2006); 10.1116/1.2216723



Frustrated by old technology? Is your AFM dead and can't be repaired? Sick of bad customer support?

It is time to upgrade your AFM
Minimum \$20,000 trade-in discount for purchases before August 31st

Asylum Research is today's technology leader in AFM

dropmyoldAFM@oxinst.com

OXFORD
INSTRUMENTS
The Business of Science®

The advertisement features three panels: an old AFM, a tombstone for 'My Old AFM 1994-2015', and a frustrated man. The background is dark blue with white and orange text.



Highly resistive epitaxial Mg-doped GdN thin films

C.-M. Lee,¹ H. Warring,¹ S. Vézian,² B. Damilano,² S. Granville,³ M. Al Khalfioui,^{2,4} Y. Cordier,² H. J. Trodahl,¹ B. J. Ruck,¹ and F. Natali^{1,a)}

¹MacDiarmid Institute for Advanced Materials and Nanotechnology, School of Chemical and Physical Sciences, Victoria University of Wellington, P.O. Box 600, Wellington, New Zealand

²Centre de Recherche sur l'Hétéro-Épitaxie et ses Applications (CRHEA), Centre National de la Recherche Scientifique, Rue Bernard Gregory, 06560 Valbonne, France

³MacDiarmid Institute for Advanced Materials and Nanotechnology, Robinson Research Institute, Victoria University of Wellington, P.O. Box 33436, Lower Hutt 5046, New Zealand

⁴University of Nice Sophia Antipolis, Parc Valrose, 06102 Nice Cedex 2, France

(Received 27 October 2014; accepted 26 December 2014; published online 12 January 2015)

We report the growth by molecular beam epitaxy of highly resistive GdN, using intentional doping with magnesium. Mg-doped GdN layers with resistivities of $10^3 \Omega \text{ cm}$ and carrier concentrations of 10^{16} cm^{-3} are obtained for films with Mg concentrations up to $5 \times 10^{19} \text{ atoms/cm}^3$. X-ray diffraction rocking curves indicate that Mg-doped GdN films have crystalline quality very similar to undoped GdN films, showing that the Mg doping did not affect the structural properties of the films. A decrease of the Curie temperature with decreasing the electron density is observed, supporting a recently suggested magnetic polaron scenario [F. Natali, B. J. Ruck, H. J. Trodahl, D. L. Binh, S. Vézian, B. Damilano, Y. Cordier, F. Semond, and C. Meyer, *Phys. Rev. B* **87**, 035202 (2013)].

© 2015 AIP Publishing LLC. [<http://dx.doi.org/10.1063/1.4905598>]

The rare-earth mononitrides (RENs) have been recognised for decades to be ferromagnetic at low temperature.^{1,2} However, their propensity for oxidation in air, combined with a tendency for the formation of nitrogen vacancies (V_N), ensured that their band structure and electron transport were poorly characterised. Even such fundamental properties as the conducting state, metal or semiconductor, have been subject to substantial experimental and theoretical disagreement.^{3–8} Recent advances in the growth and passivation of epitaxial films have begun to clarify these properties, and most of them now appear to be semiconductors.² They thus contribute new members to the relatively sparsely populated class of *intrinsic* ferromagnetic semiconductors, lending them both fundamental and technological importance with already proof of concept REN-based device structures.^{9–13} The most thoroughly studied REN is GdN, interesting for its purely spin magnetic moment in the half-filled $4f$ shell of Gd^{3+} . It has also the highest Curie temperature (T_C) of the series, reported as 70 K in most experimental studies of the past 50 years, though theoretical treatments estimate Curie temperatures that are 50% or less of the experimental values.^{14–16} However, a recent experimental report suggests that T_C has been enhanced by magnetic polarons from less than 50 K in undoped films.¹⁷ Nominally undoped epitaxial GdN thin films typically show an n-type conductivity, primarily due to doping by V_N .² A literature study shows that there is a wide range of epitaxial GdN thin films reported with electron carrier densities typically above 10^{20} cm^{-3} .^{7,8,18,19} So far, despite thin-film growth advances, it has remained difficult to reduce the concentration of V_N much below the 1% level, which dopes the films with as many as three electrons per V_N . Such relatively high V_N concentrations will remain a problem, in view of the epitaxial growth temperature,

typically above 500 °C, and the small V_N formation energy.² From a device perspective, it will be also crucial to decrease the conductivity. Here, we make important steps towards full control of the carrier concentration in GdN, demonstrating that the electron carrier density can be controlled over several orders of magnitude by Mg doping.

The GdN:Mg layers were grown by molecular beam epitaxy (MBE) on 100 nm thick wurtzite (0001) oriented high resistive AlN buffer layers, which were themselves grown by MBE on (111) silicon substrates. To prevent decomposition in air the GdN:Mg layers were capped with a 100–150 nm thick GaN layer. Atomic nitrogen species were produced by the thermally activated decomposition of ammonia (NH_3) on the growing surface, while conventional effusion cells were used for Al, Ga, Mg, and Gd solid sources. The GdN:Mg layers with thicknesses ranging from 100 nm to 140 nm were grown at a substrate temperature of $\sim 650^\circ\text{C}$ and the NH_3 and Gd beam equivalent pressures (BEPs) were 1.9×10^{-5} Torr and 5×10^{-8} Torr, respectively. The BEP of magnesium ranged from 5×10^{-11} to 6.5×10^{-8} Torr corresponding to temperatures of the Mg effusion cell between 162 °C and 300 °C. The GdN:Mg growth rate was $\sim 0.15 \mu\text{m/h}$. A typical cross-sectional scanning electron microscope (SEM) image of the structure grown is reported in Figure 1(a). The Mg concentration was determined by secondary ion mass spectrometry (SIMS). The crystalline structure was assessed by X-ray diffraction (XRD) 2θ scans and rocking curves. Electrical transport studies were carried out, including Hall effect measurements at room temperature and temperature dependent resistivity measurements performed in a closed-cycle cryostat between room temperature and 4 K. The magnetic properties of the films were investigated using a superconducting quantum interference device (SQUID) magnetometer.

The Mg concentration depth profile in the GdN layers, as measured by SIMS, is displayed in Figure 1(b). For the two

^{a)}Electronic mail: franck.natali@vuw.ac.nz

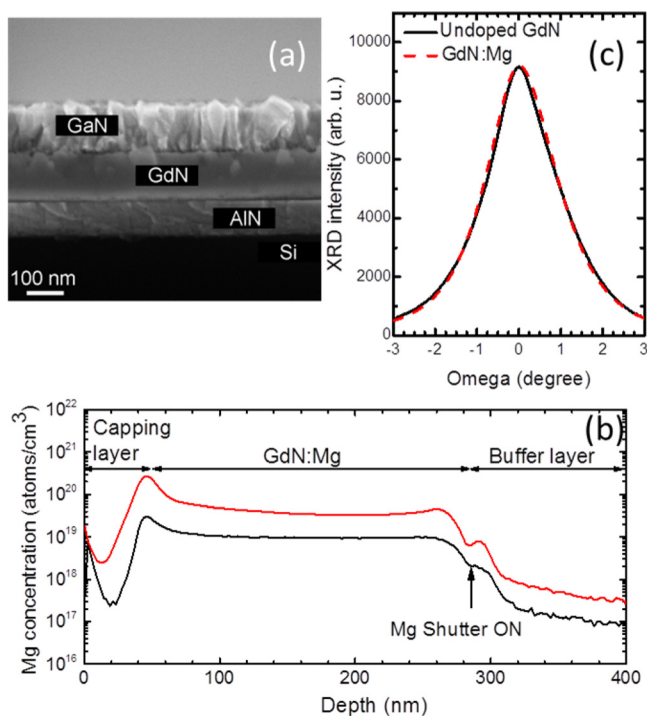


FIG. 1. (a) Cross sectional SEM image showing the grown structure. (b) SIMS profiles of Mg in GdN:Mg layers grown with Mg BEPs of 1.3×10^{-9} Torr (black) and 8.0×10^{-9} Torr (red). The measured Mg concentrations are about 1×10^{19} and 5×10^{19} atoms/cm³. (c) Rocking curves of a 140 nm thick undoped GdN layer (black line) and doped GdN layer (red dashed line) with a concentration of 5×10^{19} Mg atoms/cm³.

Mg BEPs 1.3×10^{-9} and 8.0×10^{-9} Torr, the Mg concentration was 1×10^{19} and 5×10^{19} atoms/cm³, changing as expected linearly with the incident Mg flux, or exponentially with the inverse of the effusion cell temperature. The Mg concentration has a rather flat profile, suggesting the dopant incorporation rate was constant during the growth. The upturn at the film surface is believed to be caused by incorporation of residual Mg in the chamber prior to deposition of the capping layer. The crystalline order/quality of GdN layers doped up to 5×10^{19} atoms/cm³ is very similar to that of an undoped GdN layer grown under the same conditions, as shown in Figure 1(c). The (111) XRD rocking curve full width at half maximum (FWHM) is 7200 arc sec for both a 140 nm thick Mg-doped GdN layer with a concentration of 5×10^{19} Mg atoms/cm³ and an undoped GdN layer. The FWHM of the GdN (111) reflections from $2\theta/\omega$ scans are very similar for undoped samples and samples doped up to 5×10^{19} Mg atoms/cm³. This shows that the Mg doping did not significantly affect the structural properties of the film. However, the quality of the material does start to deteriorate for a Mg BEP of 6.5×10^{-8} Torr, corresponding to a Mg concentration exceeding 2×10^{20} Mg atoms/cm³ as obtained by extrapolating the SIMS results.

Encouraged by the promising growth results, resistivity and Hall effect measurements were performed at room temperature. The efficacy of compensation by Mg can be immediately seen in the ambient-temperature electron carrier concentrations over the full range of Mg cell temperatures. The electron density of 7×10^{20} cm⁻³ for an undoped GdN layer can thus be reduced by as much as five orders of

magnitude down to $\sim 5 \times 10^{15}$ cm⁻³ for a doped GdN layer [Figure 2(a)]. For Mg concentrations above 5×10^{19} Mg atoms/cm³, the GdN:Mg films are highly resistive (>1000 Ω cm). Figure 2(b) shows that the room temperature resistivity varies inversely with the electron density over five orders of magnitude, implying an approximately constant electron mobility of ~ 5 cm²/Vs over the full range of Mg concentration.

We focus now on two films with Mg concentrations of 0 (sample H) and 10^{19} atoms/cm³ (sample M) having ambient-temperature Hall carrier concentrations of $\sim 7 \times 10^{20}$ and $\sim 5 \times 10^{16}$ cm⁻³ and ambient-temperature resistivities of 0.0024 and 25 Ω cm, respectively. Note that the concentration in the undoped film corresponds to 0.02 electrons per primitive cell, suggesting that the relatively low mobilities are due to a V_N concentration of $\sim 1\%$.

It appears at first glance improbable that a Mg concentration of 10^{19} atoms/cm³ should passivate so fully an electron concentration of nearly 10^{21} cm⁻³. It is clearly not a matter of simply compensating the V_N donors, rather it is likely that the network is altered sufficiently that there is a reduced V_N concentration when the films are grown with Mg as a dopant. Note, however, that there is recent evidence that the electrons are found in shallow traps near the V_N , forming magnetic polarons for V_N concentrations above $\sim 10^{20}$ cm⁻³.⁸ The magnetic data described below support this model.

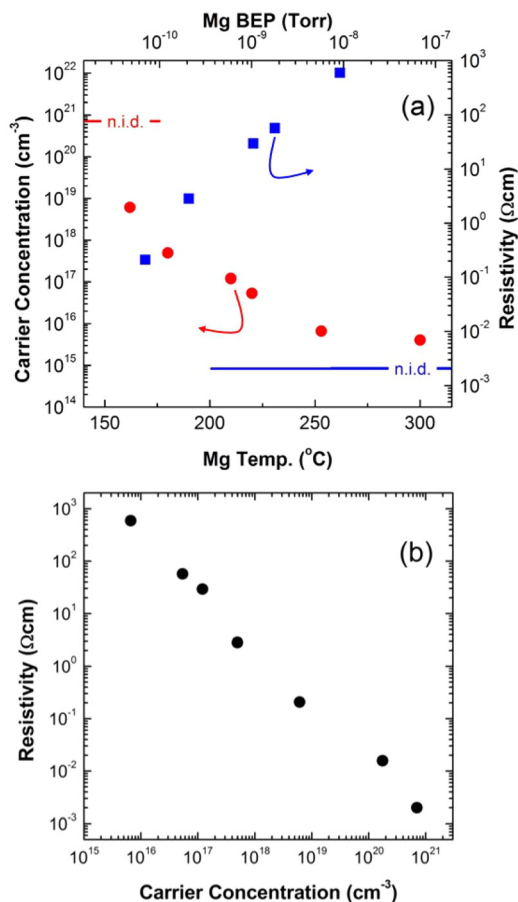


FIG. 2. (a) Electron concentration (circles) and resistivity (squares) of 100 nm thick GdN:Mg layers as a function of the Mg effusion cell temperature. The resistivity and carrier concentration for undoped GdN layers are shown by the n.i.d. lines. (b) Resistivity of 100 nm thick GdN:Mg layers as a function of the electron concentration.

The temperature dependence of the resistivities of the two films is shown in Fig. 3. The resistivity of the undoped film shows a positive temperature coefficient of resistance (TCR) near room temperature, as is commonly seen in heavily doped epitaxial GdN films. Clearly, the 0.02 electrons per primitive cell form a degenerate electron gas, though it is as yet unclear whether they reside in the conduction band (CB) or in a defect-centred tail below the CB edge. There is an anomaly peaking very close to the 70 K Curie temperature in this film (see magnetic measurements below), which is likely associated with magnetic disorder scattering.¹⁷ In contrast, the Mg doped film has not only a semiconducting magnitude of the resistance but also shows a negative TCR typical of a semiconductor but with a small activation energy. In this case, the T_C is close to 55 K (see below) and the anomaly is again found near T_C . This sample shows also a negative TCR at the lowest temperatures indicating that the ferromagnetic phase is also semiconducting.

The field-cooled (FC) magnetisation measurements in Figure 4 show that both samples are ferromagnetic at low temperature, but with substantial contrasts. The undoped film (sample *H*) (black squares) appears to transform homogeneously in the ferromagnetic phase at ~ 70 K; indeed even its paramagnetic response plotted in the inset demonstrates that homogeneous transformation, for all of the $7 \mu\text{B}$ Gd ions participate in the 70 K T_C Curie-Weiss fit. The Mg-doped film (sample *M*) also shows a very weak onset of ferromagnetism at 70 K, but in this case the majority of the Gd^{3+} ions order only at the lower Curie temperature of ~ 45 K. An analogous FC data set for a third film, with even higher Mg concentration ($5 \times 10^{19} \text{ cm}^{-3}$, i.e., a carrier concentration of $\sim 6 \times 10^{15} \text{ cm}^{-3}$) shows a further reduction in the magnetic response in the foot between 45 and 70 K, exactly as expected in the magnetic polaron scenario,^{17,20–22} while a simple T_C shift is predicted by conventional Ruderman-Kittel-Kasuya-Yosida (RKKY) treatments.²³

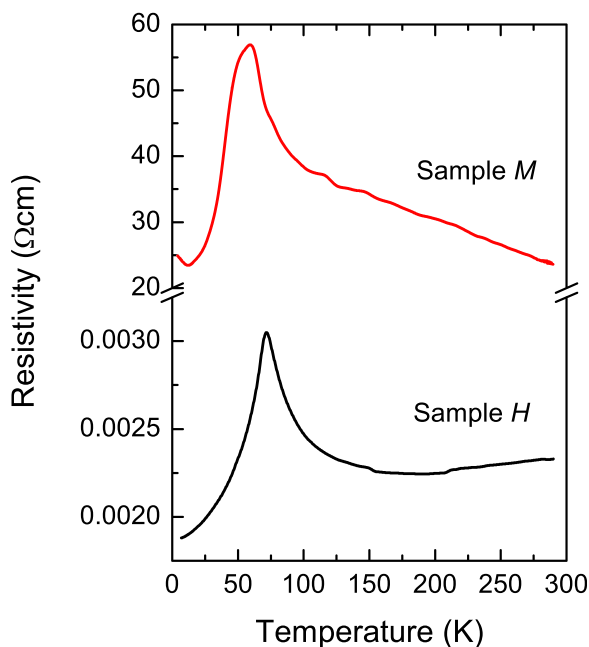


FIG. 3. Temperature dependent resistivity of an undoped GdN film (sample *H*) and a GdN:Mg layer doped with a Mg concentration of $10^{19} \text{ atoms/cm}^3$ (sample *M*).

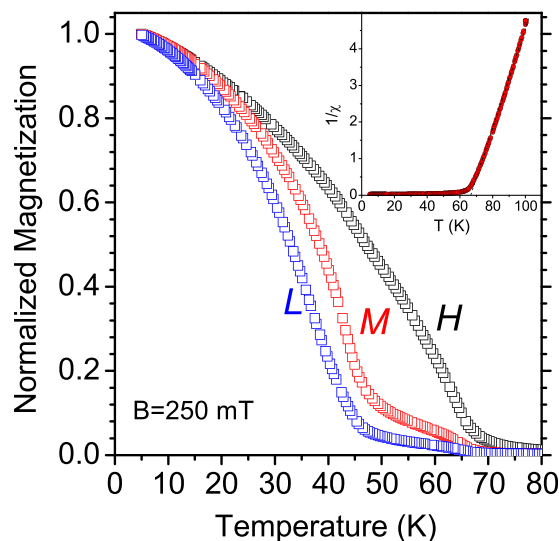


FIG. 4. Temperature dependent magnetisation of GdN films with electron carrier concentrations of $\sim 6 \times 10^{15} \text{ cm}^{-3}$ (sample *L*), $\sim 5 \times 10^{16} \text{ cm}^{-3}$ (sample *M*), and $\sim 7 \times 10^{20} \text{ cm}^{-3}$ (sample *H*). Sample *H* is an undoped sample, samples *M* and *L* correspond to GdN:Mg layers doped with a Mg concentration of 1×10^{19} and $5 \times 10^{19} \text{ atoms/cm}^3$, respectively. The inset is the temperature-dependent inverse susceptibility in an applied field of 250 mT for the undoped film (sample *H*).

In conclusion, Mg-doped GdN epilayers were grown by molecular beam epitaxy. Electrical measurements clearly show compensation of the high electron density of GdN by the introduction of magnesium atoms. No deterioration of the structural properties is observed for Mg concentration up to $5 \times 10^{19} \text{ atoms/cm}^3$. A significant reduction of the electron density down to 10^{16} cm^{-3} and increase of the resistivity up to $10^3 \Omega \text{ cm}$ is observed for a Mg concentration of $5 \times 10^{19} \text{ atoms/cm}^3$. A decrease of the Curie temperature is observed when decreasing the electron density, which is consistent with expectations from a magnetic polaron scenario.

We acknowledge funding from the Marsden Fund (Grant No. 13-VUW-1309) and the MacDiarmid Institute for Advanced Materials and Nanotechnology, funded by the New Zealand Centres of Research Excellence Fund. We acknowledge support from GANEX (ANR-11-LABX-0014). GANEX belongs to the public funded “Investissements d’Avenir” program managed by the French ANR agency.

¹F. Hulliger, *J. Magn. Magn. Mater.* **8**, 183 (1978).

²F. Natali, B. J. Ruck, N. O. V. Plank, H. J. Trodahl, S. Granville, C. Meyer, and W. R. L. Lambrecht, *Prog. Mater. Sci.* **58**, 1316 (2013).

³P. Larson, W. R. L. Lambrecht, A. Chantis, and M. van Schilgaarde, *Phys. Rev. B* **75**, 045114 (2007).

⁴C. M. Aerts, P. Strange, M. Horne, W. M. Temmerman, Z. Szotek, and A. Svane, *Phys. Rev. B* **69**, 045115 (2004).

⁵C.-G. Duan, R. F. Sabiryanov, J. Liu, W. N. Mei, P. A. Dowben, and J. R. Hardy, *Phys. Rev. Lett.* **96**, 139901 (2006).

⁶H. J. Trodahl, A. R. H. Preston, J. Zhong, B. J. Ruck, N. M. Strickland, C. Mitra, and W. R. L. Lambrecht, *Phys. Rev. B* **76**, 085211 (2007).

⁷M. A. Scarpulla, C. S. Gallinat, S. Mack, J. S. Speck, and A. C. Gossard, *J. Cryst. Growth* **311**, 1239 (2009).

⁸R. Vidyasagar, T. Kita, T. Sakurai, and H. Ohta, *Appl. Phys. Lett.* **102**, 222408 (2013).

⁹K. Senapati, M. G. Blamire, and Z. H. Barber, *Nat. Mater.* **10**, 849 (2011).

¹⁰M. G. Blamire, A. Pal, Z. H. Barbe, and Kartik Senapati, *Proc. SPIE* **8461**, Spintronics V, 84610J (2012).

- ¹¹H. Warring, B. J. Ruck, H. J. Trodahl, and F. Natali, *Appl. Phys. Lett.* **102**, 132409 (2013).
- ¹²S. Krishnamoorthy, T. Kent, J. Yang, P. S. Park, R. C. Myers, and S. Rajan, *Nano Lett.* **13**, 2570 (2013).
- ¹³A. Kandala, A. Richardella, D. W. Rench, D. M. Zhang, T. C. Flanagan, and N. Samarth, *Appl. Phys. Lett.* **103**, 202409 (2013).
- ¹⁴D. X. Li, Y. Haga, H. Shida, T. Suzuki, Y. S. Kwon, and G. Kido, *J. Phys.: Condens. Matter* **9**, 10777 (1997).
- ¹⁵C.-G. Duan, R. F. Sabiryanov, W. N. Mei, P. A. Dowben, S. S. Jaswal, and E. Y. Tsymbal, *Appl. Phys. Lett.* **88**, 182505 (2006).
- ¹⁶C. Mitra and W. R. L. Lambrecht, *Phys. Rev. B* **78**, 134421 (2008).
- ¹⁷F. Natali, B. J. Ruck, H. J. Trodahl, D. L. Binh, S. Vézian, B. Damilano, Y. Cordier, F. Semond, and C. Meyer, *Phys. Rev. B* **87**, 035202 (2013).
- ¹⁸F. Natali, N. O. V. Plank, J. Galipaud, B. J. Ruck, H. J. Trodahl, F. Semond, S. Sorieul, and L. Hirsch, *J. Cryst. Growth* **312**, 3583 (2010).
- ¹⁹F. Natali, S. Vézian, S. Granville, B. Damilano, H. J. Trodahl, E.-M. Anton, H. Warring, F. Semond, Y. Cordier, S. V. Chong, and B. J. Ruck, *J. Cryst. Growth* **404**, 146 (2014).
- ²⁰A. Mauger and C. Godart, *Phys. Rep.* **141**, 51 (1986).
- ²¹P. Liu and J. Tang, *Phys. Rev. B* **85**, 224417 (2012).
- ²²M. Arnold and J. Kroha, *Phys. Rev. Lett.* **100**, 046404 (2008).
- ²³A. Sharma and W. Nolting, *Phys. Rev. B* **81**, 125303 (2010).